Original Article

Three-dimensional evaluation of the intensity of land use changes (case study: Kardeh watershed, Iran)

Mehdi Mehdizadeh Karizaki[1], Amin Alizadeh[2]*, Hosein Ansari[2], Hadi Memarian Khalil Abad[3]

[1] PhD. student, Irrigation and drainage engineering, Ferdowsi University of Mashhad, Mashhad, Iran. [2] Professor, Faculty of agriculture, Ferdowsi University of Mashhad, Mashhad, Iran. [3] Associate Professor, Faculty of natural resources and environment, University of Birjand, Iran.

Correspondence: Amin Alizadeh; Professor, Faculty of agriculture, Ferdowsi University of Mashhad, Mashhad, Iran. E-mail: alizadeh@gmail.com

ABSTRACT

Unmanaged land use change is one of the major challenges of natural resources in the 21st century. The arid and semi-arid watersheds in Iran are faced with this problem, as well. This work analyzes the size and intensity of land use changes and the stationary at three levels of time, category and transition intensity in the Kardeh dam watershed, northeastern Iran. With the field investigations and the existing land use maps, the study area was classified into the five categories, including rangeland, irrigated farming and orchards, rainfed farming, bareland and residentia . The intensity analysis was done based on a mathematical method that compared the observed intervals. A cross-tabulation matrix was created for each time interval (1987-1998, 1998-2008, 2008-2016) and the intensity of changes was examined at the three levels of time interval, category intensity, and transition intensity. The largest amount of land use change is occurred in the first time period (1987-1998), however, the intensity of the changes in the last time period (2008-2016) includes the highest amount. Intense and unprincipled changes of rangelands to irrigated and rainfed farming has led to an increased intensity of bareland changes. The results illustrate that the most changes and fluctuations are among the rangeland, irrigated and rainfed farming categories without a regular pattern. Rangeland is the only dormant category for both gains and losses, in spite of being involved in most of the changes.

Keywords: Land use change, category, three-dimensional intensity analysis, classification

Introduction

Iran is located in the arid and semi-arid regions of the earth; therefore, dryness is one of the most prominent features of this country and no region can be found, that is not affected by the drought and its effects [1]. More than two-third of Iran has arid and semi-arid climate and naturally a fragile ecosystem. However, there has been an upward trend in the degradation of natural resources and desertification in many areas of Iran due to some factors such as the population growth, uncontrolled groundwater use, excessive grazing, land use change and industrial development and this has endangered the sustainability of these areas. Proper management of these regions requires national determination and a careful and comprehensive planning [2].

Water is considered as one of the most valuable natural resources of a country and the economic and social benefits derived from its proper use are of great importance. Population growth along with the lack of a proper planning for the productivity of land has led to the destruction of forests and pastures or their use as the agricultural lands. Consequently, less water penetrates the soil in the upstream of rivers and it flows faster towards the plain. As a result, floods are more abundant, more severe, and more people are damaged by them. Undoubtedly, the presence of vegetation in the basin is considered as an effective factor in the reduction of flood proneness due to its effects in the hydrological cycle [3].

Unmanaged land use change is one of the major challenges of the 21st century. In general, three primary features of the catchment area, including the soil, vegetation, and topography, operate the hydrological changes in the form of the rainfall-runoff and erosion processes. The hydrological effects of land use and vegetation management are evident in the changes in runoff depth, minimum discharge, maximum discharge, soil moisture, and evapotranspiration [4]. Land use changes are the

Access this article online	
Website: www.japer.in	**E-ISSN:** 2249-3379

How to cite this article: Mehdi Mehdizadeh Karizaki, Amin Alizadeh, Hosein Ansari, Hadi Memarian Khalil Abad. Three-dimensional evaluation of the intensity of land use changes (case study: Kardeh watershed, Iran). J Adv Pharm Edu Res 2020;10(S2):157-170.
Source of Support: Nil, Conflict of Interest: None declared.

result of a complex interaction between the physical, biological, economic, and social indicators and directly affect the increased level of surface runoff [5]. Land use changes are recognized as one of the main drivers of the hydrological changes in the catchment area [6].

Human intervention in the basins is among the most important factor affecting land use changes, which is associated with the change in the quantitative and qualitative characteristics of runoff in rivers [7]. With the development of urban lands, the level of impervious lands is expanding rapidly, the rainfall infiltration is decreasing and the runoff coefficient is increasing. Land use changes and expansion of urbanization increase the risk of flooding due to the increased discharge volume and also decrease the time discharge reaches the peak [8]. Brun and Band (2002) evaluated the impact of land use change and development of urban areas on the hydrologic behavior of basins in the United States [9]. The results indicated that the change in the land use has caused a decrease of about 20% in the discharge of the basins. Land use in the catchment areas affects the quality of water from uncertain sources and the highest rate of pollution is caused by the increased land use changes [10]. Land use changes may bring some problems in the region's climate, water cycle, and its natural habitat [11]. Every year, population growth combined with the increased demand for lands in order for agricultural and housing purposes and the industrial development cause the loss of fertile lands and changes in the water balance of the region [12]. Land use changes along with the increased urbanization, agricultural activities, and forest degradation are among the major drivers of changes in the water balance [13]. Land use changes affect water quality through increasing the concentration of nitrogen and phosphate compounds due to the increased agricultural and biological activities [14]. Human activities and natural phenomena such as droughts and floods lead to changes in the land coverage and land use, and this may have severe environmental, social, economic, and political consequences [15]. Finding the process and pattern of the coverage and land-use changes is the main focus of researches examining the human and natural interactions on the local and global scales [16]. The usual strategy for analyzing the spatial distribution of land use changes is first to identify the pattern of quantitative and qualitative changes, and then change processes are examined [17]. An estimation of the future prospect of land use changes would be an effective step in the sustainable water resources management to deal with the crises caused by the overdevelopment of land uses [18]. Land cover maps play an essential role in the analysis of land use changes [19]. As land-use changes occur at a widespread and expansive level, remote sensing technology is an indispensable tool in assessing changes due to the frequent and repeated coverage of the earth [20]. To obtain information about the land cover and land use, remote sensing data are available with spatial, temporal, spectral, and radiometric separations [21].

From the studies conducted by Memarian et al. (2013) in the catchment areas of Malaysia, they concluded that land use changes are occurring at a rapid pace [22]. To examine and monitor the land use changes, the best way to quantify changes among the uses between the two nodes is to use the transition matrix [23]. Pontius and Malaysia (2004) have invented a class size-based approach to assess the relative intensity of land use changes, which can be used for all types of uses [24]. Nowadays, many researchers use the assumptions and innovative method of Pontius and Malizia (2004) to analyze their research results. Huang et al. (2007) used the intensity analysis to study the pattern of temporal and spatial variations in the land cover and land use in the catchment basin of Jiulong River in China [25]. Aldwaik and Pontius (2012) [26] expanded this method for the analysis of the intensity of changes to investigate the changes at three levels (1) time level land use changes; (2) the level of gain and loss for each category level; and (3) the intensity of land use changes and their transition from one level to another. The land use change analysis over the time is the highest level of the application of this method [27]. The intensity analysis is a quantitative form for calculating the differences between the classes and it is summarized in a transition square matrix with rows and columns having the same levels. With the analysis of intensity in each level, the degree of deviation between the observed changes and the assumed level of intensity can be obtained [26].

This study was conducted with the aim of a quantitative detection of land use changes in the watershed of Kardeh Dam located in Mashhad, Iran. Mashhad, with a total area of 3,288 square kilometers and 3 million inhabitants, is the second largest and populated city in Iran (Population and Housing Census, 2016). The increased and unplanned development of this metropolis and the establishment of industries in Mashhad plain have led to the change in the land use of all plain watersheds, which is not consistent with the existing water resources, and has created serious risks for the management of this city.

Kardeh Dam watershed, with an area of about 54,710 hectares in northeastern Iran, is located in 42 kilometers of the north of Mashhad (the second largest metropolis of Iran). This watershed supplies a part of the drinking water of Mashhad and also irrigates agricultural lands located in the lower areas of Kardeh Dam [28]. In recent years, this basin has faced with a dramatic reduction in runoff due to the land use and land cover changes with the development of gardens and agricultural lands, and uncontrolled water withdrawal from the surface and underground resources. With the reduced water yield of the river of Kardeh, it has faced a sharp decline in the reservoir level, and this has caused severe problems in supplying the city's drinking water resources and water for the agricultural lands in the downstream of the dam. Therefore, the present study aims to investigate the land use changes in this basin in different categories and time periods at two spatial and temporal dimensions and in three levels of time, category level, and intensity based on the method presented by Aldwaik and Pontius (2012).

Materials and Methods

Studiy Area

The Kardeh Dam watershed with an area of about 54,425 hectares in northeastern Iran is located in 42 kilometers of the north of Mashhad. This region is on the southern slopes of Hezar Masjed Mountains and Kopet Daq geology zone in the coordinates of 59°26' 3" to 59°44' 48" Eastern longitude and "17'37°36 to 25'58°36 North latitude (36°37'53"N 59°39'55"E) (Figure 1). The most important river of this watershed is Kardeh which is shaped by the interconnection of the two branches of the Koshkabad and AL Rivers. Kardeh Dam has been built at the end of the basin to provide part of Mashhad drinking water and also irrigate downstream agricultural lands with a capacity of 38 million cubic meters. Kardeh basin is a mountainous area and it has slopes with a fairly steep hillside and the highest point is in the altitudes of Hezar Masjed with the height of 2948 meters and the lowest point of the basin in the Kardeh dam with a height of 1291 meters and an average elevation of 2004 meters above the sea level. Its general shape is like a rectangular and the general slope of the area is 34% and the catchment circumference is about 117 km. Kardeh Basin includes 13 villages whose main economic activity is animal husbandry, gardening, and agriculture [28].

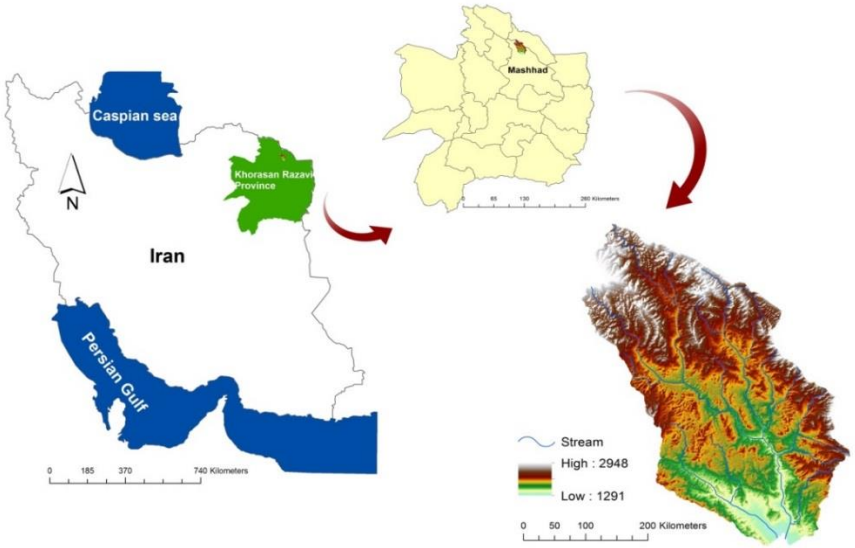

Figure 1. Geographic location of study area

Methodology

In this study, the spatial data obtained from the satellite images of TM (Landsat 5 Thematic Mapper) and LDCM (Landsat Data Continuity Mission) were used to extract land use data. The Landsat 5 satellite shoots in bands blue, green, red and near infrared with a spatial resolution of 30 meters and a thermal band with a spatial resolution of 120 meters [29]. The Landsat 8 satellite has two sensors: the Operational Land Imager (OLI) and the Thermal Infrared Sensor (TIRS); these two sensors together make up 11 bands; 8 bands have a resolution of 30 meters, a 15-meter panchromatic band, and two 100-meter thermal bands [30].

Among the important criteria in choosing the type of satellite for the present study are the proper sensor, appropriate spatial, temporal, and spectral resolution, and lack of the problem of the presence of clouds in the region [31]. To study the land cover and land use changes in the Kardeh basin, a 30-year time span was considered during the three decades of 1987 to 1998, 1998 to 2008, and 2008 to 2016, respectively. Satellite images related to the beginning of every decade, obtained from the Landsat 5 and 8 satellite archives and the TM and OLI sensors, were prepared and analyzed (https://earthexplorer.usgs.gov). The best time for choosing satellite images is the summer when there is full vegetation and the degree of cloudiness for images is zero percent. The specifications of the satellite imagery used in this study are presented in Table 1.

Radiometric correction is applied to reduce or eliminate the two major atmospheric and device errors. The atmospheric error (haze) appears as an accumulative error, causing over clarity of the image, and reduces the contrast and resolution in the image. In the provided images, the dark subtraction technique was applied in order for the atmospheric correction [32]. After processing the satellite images through some stages including the image mosaicking, making color composites radiometric and geometric correction, the images were classified using the Fuzzy-Maximum Likelihood technique (Fuzzy-ML). The Maximum Likelihood (ML) approach has been widely used since 1980 to extract thematic information [33].

Table 1. Satellite images characteristics

Row	Date	Satellite Name	Sensor Name	Band names of electromagnet used in spectral resolution

1	22 Sep 1987	Landsat 5	TM	Band1=Blue , Band2=Green , Band3=Red , Band4=Near Infrared(NIR) , Band5=Shortwave Infrared (SWIR 1) , Band7=Shortwave Infrared (SWIR 2)
2	18 Jul 1998	Landsat 5	TM	Band1=Blue , Band2=Green , Band3=Red , Band4=Near Infrared(NIR) , Band5=Shortwave Infrared (SWIR 1) , Band7=Shortwave Infrared (SWIR 2)
3	13 Jul 2008	Landsat 5	TM	Band1=Blue , Band2=Green , Band3=Red , Band4=Near Infrared(NIR) , Band5=Shortwave Infrared (SWIR 1) , Band7=Shortwave Infrared (SWIR 2)
4	17 Jun 2016	Landsat 8	OLI	Band1=Ultra Blue , Band2=Blue , Band3=Green , Band4=Red , Band5=Near Infrared(NIR) , Band6=Shortwave Infrared (SWIR 1) , Band7=Shortwave Infrared (SWIR 2)

Maximum likelihood method (MLC)

One of the most common methods to categorize land cover is the supervised MLC method [34, 35]. The algorithm of this method is according to the likelihood of assigning a pixel to the target class [23]. In the original equation, it is supposed that all classes are similar in terms of this likelihood and the distributions of all bands are normal. The following main equation is usually used for the MLC:

$$g_i(x) = \ln(a_c) - [0.5\ln(|cov_c|)] - [0.5(x - M_c)^T(cov_c^{-1})((x - M_c))] \quad (1)$$

Where, c represents the desired class, x shows an n-dimensional data (where n indicates the number of bands), ac shows the possibility of belonging a pixel to the class c that, by default, it is supposed to be the same for all classes. Covc and Mc are determinant of covariance matrix and mean vector of class c, respectively. The ln denotes the natural logarithm and transposition function is indicated by T [32, 35, 36].

Fuzzy classification

To categorize land use, the two methods of fuzzy and maximum likelihood were combined in this method. The theory of probability states that if the event A shows a set of elements in a large set (φ), then, the probability density function of A, i.e. P(A) is determined as follows [37, 38]:

$$P(A) = \int_{\varphi} H_A \cdot (S) \quad (2)$$

Where, S shows an element in the set φ and H_A denotes the hard membership function. For image classification, event A is a class or cluster and S shows the phenomenon measure vector in a pixel, i.e. Digital Number (DN). H_A membership function indicates if S belongs to the class A (membership grade equal to one) or not (membership grade equal to zero) [37]. If A is considered as a fuzzy event and a fuzzy subset of set φ, the probability density function of A will be equal to the following [37]:

$$P(A) = \int_{\varphi}^{A} \mu_A . (S) \quad (3)$$

Where, μ_A denotes membership function. Generally, this method is applied together with conventional classification approaches such as the minimum distance or maximum likelihood. Hence, spectral distance and classified maps determined by traditional methods with a weight matrix are fed into the system and then each pixel is introduced into multiple classes by the application of fuzzy algorithm on the classified image. Finally, each pixel is classified into a certain class by applying the weight coefficient matrix and convolution method [19, 38]:

With the field investigations and the existing land use maps, the study area was classified into the 5 category as described in Table 2.

Table 2. Classification of land cover and land use in

Category No.	Description	Category Name
1	Rangeland	PAST
2	Irrigated farming and orchards	ORCD
3	Rainfed farming	AGRL
4	Rock outcrop – Bareland	BARR
5	Residential	URML

After defining land uses with the help of points registered at the field investigation stage, the pixels on color images representing the reflection of the intended use or coverage were selected. The pixels were selected in a way that the pixel sets of each training site only include the pixels of a particular use. In choosing the educational samples, it was tried to have a good level of dispersion and to be a good indication for the considered category levels.

To provide the ground truth map, the random samples were used; the accuracy of maps was evaluated through the pixel to pixel comparison of the classified maps with the ground truth. Ground control points were considered in a way that to be scattered throughout the image; more points were considered on the edges and less points in the areas where the type of land use was simple and with a little change. In order to evaluate the accuracy of classified images, an error matrix was created through matching the classified maps with the ground truth maps and field studies. Accordingly, the overall accuracy, producer's accuracy, user's accuracy [39], and kappa coefficient were calculated. The kappa coefficient (k) was used to summarize the information generated by the error matrix [40].

After classification of the images, their changes were investigated over the time periods from 1987 to 1998, 1998 to 2008, and 2008 to 2016 at the three levels of time interval, category, and transition. At each level, the stationary patterns of land use were compared at different time intervals. Stationary means that the pattern of change in land use at a time interval is similar to the pattern of change in the other interval or time period. In the case of land gain at the category level, the stationary means that the intensity of increase in the area of land is larger or smaller than the uniformity line of the intensity of changes in all the time periods of the study. This is also true about the loss of land areas. In this case, this category level of use is defined to be constant in terms of the increase or decrease in the area. Moreover, in the analysis of the intensity of changes, if class n changes to class m in all time periods, or it does not change in all intervals of study, then this kind of conversion from n to m is also defined to be constant [41].

The intensity analysis is done based on a mathematical method that compares the observed temporal intensities with the uniform intensity. In this study, a cross-tabulation matrix was created for each time interval and the intensity of changes was examined at the three levels of time interval, category intensity, and transition intensity. Time interval level shows the overall land use changes over the time in each time interval. At this level, the intensity of observed annual variations is compared with the uniform rate of changes. The category intensity level shows the intensity of category and the amounts of gain and loss for each category level. The transition intensity level represents the intensity of changes and transition from one category level to another [42].

Intensity calculation:

Aldwaik and Pontius (2012) presented the following methods to compute intensities of transitions

1. Time intensity

To determine the time intensity, the following equations are applied

$$U = \frac{100\times\sum_{t=1}^{T=1}\left\{\sum_{i=1}^{J}\left[\left(\sum_{i=1}^{J} C_{tij}\right)-C_{tij}\right]\right\}/\left\{\sum_{j=1}^{J}\left(\sum_{i=1}^{J} C_{tij}\right)\right\}}{Y_T-Y_1} = \frac{100\times area\ of\ change\ during\ all\ intervals/area\ of\ study\ region}{duration\ of\ all\ intervals} \quad (4)$$

and,

$$S_t = \frac{100\times\left\{\sum_{j=1}^{J}\left[\left(\sum_{i=1}^{J} C_{tij}\right)-C_{tjj}\right]\right\}/\left\{\sum_{j=1}^{J}\left(\sum_{i=1}^{J} C_{tij}\right)\right\}}{Y_{t+1}-Y_t} = \frac{100\times area\ of\ change\ during\ interval\ [Y_t.Y_{t+1}]/area\ of\ study\ region}{duration\ of\ interval\ [Y_t.Y_{t+1}]} \quad (5)$$

where: U denotes the value of uniform line for time intensity analysis and St represents the length of bar for the interval [Y_t, T_{t+1}]. J indicates the number of categories (≥ 2), i shows the index for a category (= 1, 2, … , J), j represents the index for a category (= 1, 2, … , J), m indicates an index for the losing category in transition of interest, n shows an index for the gaining category in transition of interest, T shows the number of time points (≥ 2), t shows an index for a time point (= 1, 2, … T), Y_t denotes the year at the time point t and C_{tij} represents the number of cells transiting from category i at time Y_t to category j at time Y_{t+1} [26].

2. Category Intensity

To determine the intensity metrics for the category level the following equations are applied:

$$P_t = \frac{100\times\left\{\sum_{j=1}^{J}\left[\left(\sum_{i=1}^{J} C_{tij}\right)-C_{tjj}\right]\right\}/\{Y_{t+1}-Y_t\}}{\sum_{j=1}^{J}\left(\sum_{i=1}^{J} C_{tij}\right)} = \frac{100\times area\ of\ change\ during\ interval\ [Y_t.Y_{t+1}]/duration\ of\ interval\ [Y_t.Y_{t+1}]}{area\ of\ study\ region} \quad (6)$$

$$L_{ti} = \frac{100\times\left\{\left(\sum_{j=1}^{J} C_{tij}\right)-C_{tii}\right\}/\{Y_{t+1}-Y_t\}}{\sum_{j=1}^{J} C_{tij}} = \frac{100\times area\ of\ gross\ loss\ of\ category\ i\ during\ [Y_t.Y_{t+1}]/duration\ of\ interval\ [Y_t.Y_{t+1}]}{area\ of\ category\ i\ at\ time\ Y_t} \quad (7)$$

$$G_{tj} = \frac{100\times\left\{\left(\sum_{i=1}^{J} C_{tij}\right)-C_{tjj}\right\}/\{Y_{t+1}-Y_t\}}{\sum_{i=1}^{J} C_{tij}} = \frac{100\times area\ of\ gross\ gain\ of\ category\ j\ during\ [Y_t.Y_{t+1}]/duration\ of\ interval\ [Y_t.Y_{t+1}]}{area\ of\ category\ j\ at\ time\ Y_{t+1}} \quad (8)$$

where: P_t shows the value of uniform line for time interval [Y_t, Y_{t+1}], Lti denotes the length of bar for time interval [Y_t,Y_{t+1}] for gross loss of category i, and G_{tj} represent the length of bar for time interval [Y_t,Y_{t+1}] for gross gain of category j [26].

3. Transition Intensity

Investigating the transition intensity yields useful information on the transition intensity from the category m to another category n. To this aim, first, we must examine the gain pattern of category n, then the loss pattern of the category m. Equations 9 and 10 indicate which other categories strictly avoid targeting the category n. Equation 9 shows the observed intensity to the category n from each category i (i <> n). Equation 9 generates the number (J-1) intensity at each time interval, i.e., one intensity for each non-category n in each time interval. For each time period, equation (10) generates a uniform intensity for the category n, which defines the intensity of the annual transfer to the category n, assuming that the category n uniformly gains among the other categories. The uniformity intensity gained by the equation 10 is the mean weighted of the intensity (J-1) generated by equation (9), where the weight of each category i is of the area i of the category i in the time interval Yt. In analyzing the intensity of the transition changes to investigate the staticity from m to n, if the category n changes to the category m in all c or vice versa if it does not change in all time slots of the study, this type of transition from n to m is also defined as stationary [26].

$$R_{tin} = \frac{area\ of\ transition\ from\ i\ to\ n\ during\ [Y_t.Y_{t+1}]/duration\ of\ [Y_t.Y_{t+1}]}{area\ of\ category\ i\ at\ time\ Y_t} \times 100\% = \frac{C_{tin}/(Y_{t+1}-Y_t)}{\sum_{j=1}^{J} C_{tij}} \times 100\% \quad (9)$$

$$W_{tn} = \frac{area\ of\ gross\ gain\ of\ category\ n\ during\ [Y_t.Y_{t+1}]/duration\ of\ [Y_t.Y_{t+1}]}{area\ that\ is\ not\ category\ n\ at\ time\ Y_t} \times 100\% = \frac{\left[\left(\sum_{i=1}^{j} C_{tin}\right)-C_{tnn}\right]/(Y_{t+1}-Y_t)}{\sum_{j=1}^{j}\left[\left(\sum_{i=1}^{j} C_{tij}\right)-C_{tnj}\right]} \times 100\% \quad (10)$$

In order to analyze the transition intensity for each time interval, two output sets are developed, one of which pertains to obtaining the category n, and another to losing the category m. Equations 11 and 12 also indicate loss rates. In other words, equations 11 and 12 define which other categories will avoid "targeting" of the category m. Equations 11 and 12 are applied for this fact that if the category m exists at the end of a period in a definite position, then it cannot be removed from that location during that time interval. Equation (11) indicates the transition intensity of the observation from the category m to each category J (m <> J). Equation (11) generates a number of J-1 intensity at each time interval. Equation 12 has only one output, which is defining the annual uniformity of the category m to each other categories in each time interval. The uniform intensity depicts conditions that the category m belongs to the other categories where all categories except the category m lose each one in proportion to their size from the category m [26].

$$Q_{tmj} = \frac{area\ of\ transition\ from\ m\ to\ j\ during\ [Y_t.Y_{t+1}]/duration\ of\ [Y_t.Y_{t+1}]}{area\ of\ category\ j\ at\ time\ Y_{t+1}} \times 100\% = \frac{[C_{tmj}/(Y_{t+1}-Y_t)]}{\sum_{i=1}^{J} C_{tij}} \times 100\% \quad (11)$$

$$V_{tm} = \frac{area\ of\ gross\ loss\ of\ category\ m\ during\ [Y_t.Y_{t+1}]/duration\ of\ [Y_t.Y_{t+1}]}{area\ that\ is\ not\ category\ m\ at\ time\ Y_{t+1}} \times 100\% = \frac{\left[\left(\sum_{j=1}^{j} C_{tmj}\right)-C_{tmm}\right]/(Y_{t+1}-Y_t)}{\sum_{i=1}^{j}\left[\left(\sum_{j=1}^{j} C_{tij}\right)-C_{tim}\right]} \times 100\% \quad (12)$$

In the above formulas, provided for the calculation of intensity at three levels, the letters and markings are as follows in table 3.

Table 3. Letters and markings

J number of categories;
i index for a category at the initial time for a particular time interval;
j index for a category at the final time for a particular time interval;
m index for the losing category in the transition of interest;
n index for the gaining category in the transition of interest;
T number of time points;
t index for initial time point of interval [Yt , Yt+1], where t ranges from 1 to T-1;
Y_t Year at time point t;
C_{tij} number of pixels that transition from category I at time Yt to category j at time Yt+1;
S_t annual intensity of change for time interval [Yt , Yt+1];
U value of uniform line for time intensity analysis;
G_{tj} annual intensity of gross gain for time interval [Yt , Yt+1];
L_{ti} annual intensity of gross loss of category ,i for time interval [Yt , Yt+1];
R_{tin} annual intensity of gross loss of transition from category ,i to category n during time interval [Yt , Yt+1]; where ,i≠ n
W_{tn} value of uniform intensity of transition to category n from all non- n categories at time Yt during time interval [Yt , Yt+1];
Q_{tmj} annual intensity of transition from category m to category j during time interval [Yt , Yt+1]; where j≠ m;
V_{tm} value of uniform intensity of transition from category m to all non- m categories at time Yt+1 during time interval [Yt , Yt+1];

Results and Discussion

Accuracy assessment of land use classification

Figure 2 indicates land use maps after applying the fuzzy-ML algorithm on satellite images. This figure indicates the land use classifications of the Kardeh Dam basin in 1987, 1998, 2008, and 2016.

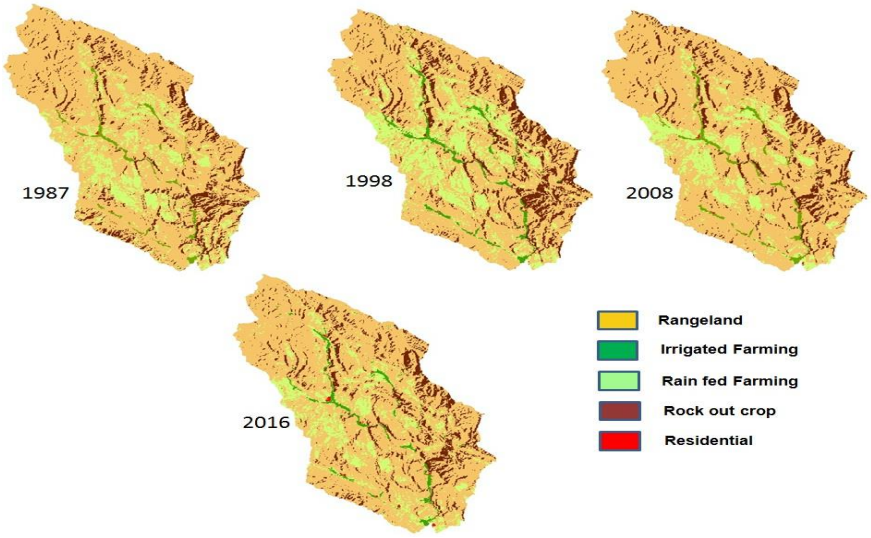

Figure 2. Land use classification maps of the Kardeh Dam basin in 4 time intervals

Table 4 indicates the results of the error of land use classification and its correspondence with ground truth in each time interval. In this Table, the general accuracy, Kappa coefficient, producer's accuracy and user accuracy were calculated [39]. The zero value in the Kappa criterion indicates that there is no agreement between the information derived from the classification and the information of ground truth. While the kappa criterion value completely represents the information derived from the classification and the ground truth information [40]. Based on the results presented in Table 4, the Kappa coefficient calculated for all time periods is in an appropriate range, and do not have a significant difference. Evaluation of the classification accuracy indicates the low level of accuracy of the producer's on the BARR category in 2008, which is 77%. Other criteria have acceptable values [43].

Table 4. Classification Results

Time Intervals	Overall Classification Accuracy (%)	Overall Kappa Statistics	Categories	Producers Accuracy (%)	Users Accuracy (%)
1987	98	0.92	PAST	99	99
			ORCD	100	100
			AGRL	100	89
			BARR	86	100
			URML	100	100
1998	98	0.95	PAST	100	97
			ORCD	100	100
			AGRL	100	100
			BARR	84	100
			URML	100	100
2008	95	0.90	PAST	100	96
			ORCD	100	100
			AGRL	100	92
			BARR	77	100
			URML	100	100
2016	97	0.92	PAST	100	97
			ORCD	100	100
			AGRL	90	100
			BARR	83	100
			URML	100	100

Assessment of land use / cover changes

Figure 3 presents the rate and intensity of changes in the time slots 1987-1998, 1998-2008, and 2008-2016. The left diagram indicates the area and the right diagram indicates the intensity of changes.

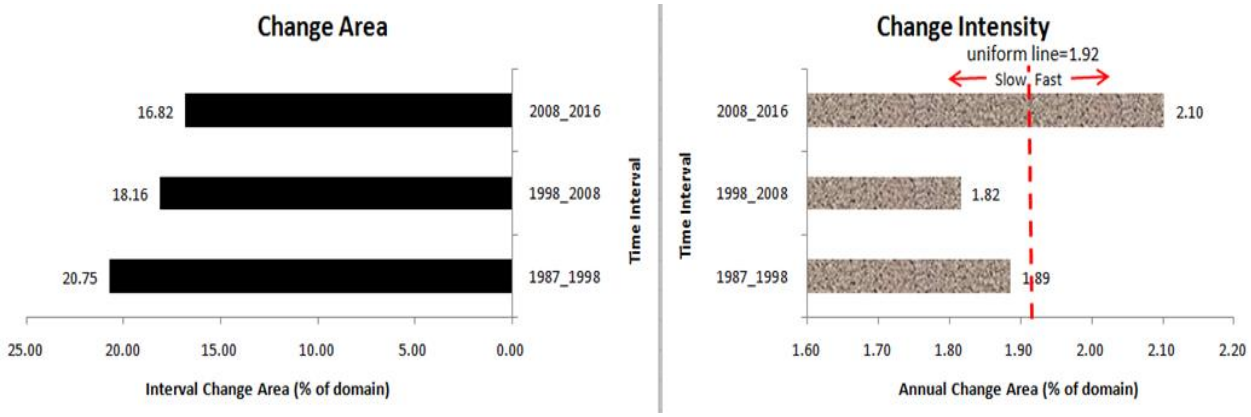

Figure 3. Interval intensity analysis across three time intervals

As seen in the Figure 3, the Kardeh Dam basin accounts for the largest amount of land use change in the period 1987-1998, however, the intensity of the changes in the period 2008-2016 includes the highest amount. The intensity of the changes in the periods 1987-1998 and 1998-2008, placed before the uniform line, indicates a slow change in the land use during those intervals. Conversely, the intensity of the change over the period of 2008-2016, which cut the uniform line, indicates quick changes in land use during this period, which is mainly due to the rapid growth of urbanization and increased migration to the central city of Mashhad during this period. The rapid growth of urbanization and increased demand for food has caused rapid changes in the land use in adjacent basins, which could justify the increasing land use changes in the studied area [44].

Figure 4 illustrates the intensity of categorical land use changes. As seen, in all time slots, Rangeland and Rainfed Farming have the most changes compared to the entire period.

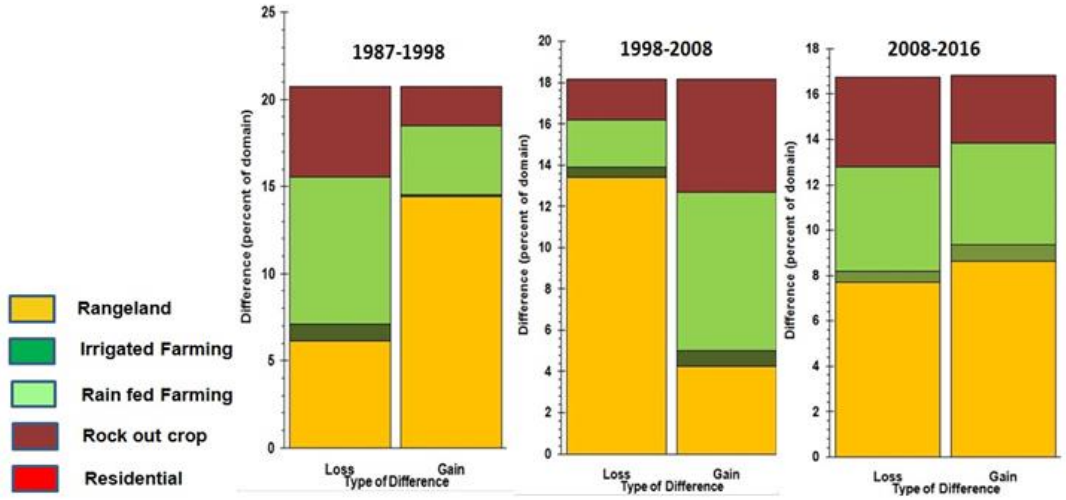

Figure 4. Categorical intensity analysis of land use changes across three time intervals

During period 1987-1998, the highest gain pertained to the Rangeland category and the highest loss pertained to rainfed farming. During this period, the intensity of the loss of the Irrigated Farming category is also higher than its gain. During the time interval 1998-2008, Rangeland category accounted for the highest loss and the rainfed Farming for the highest gain. During this time, Irrigated Farming was not changed a lot. In the period 2008-2016, the intensity of gain and loss has a slight change, however, the highest gain pertains to the rangeland and the highest loss pertains to the rainfed Farming category, which can mainly be due to a decrease in rainfall and recent droughts [45].

Figure 5 presents the stationary intensity of the categories at any time interval compared to gain and loss.

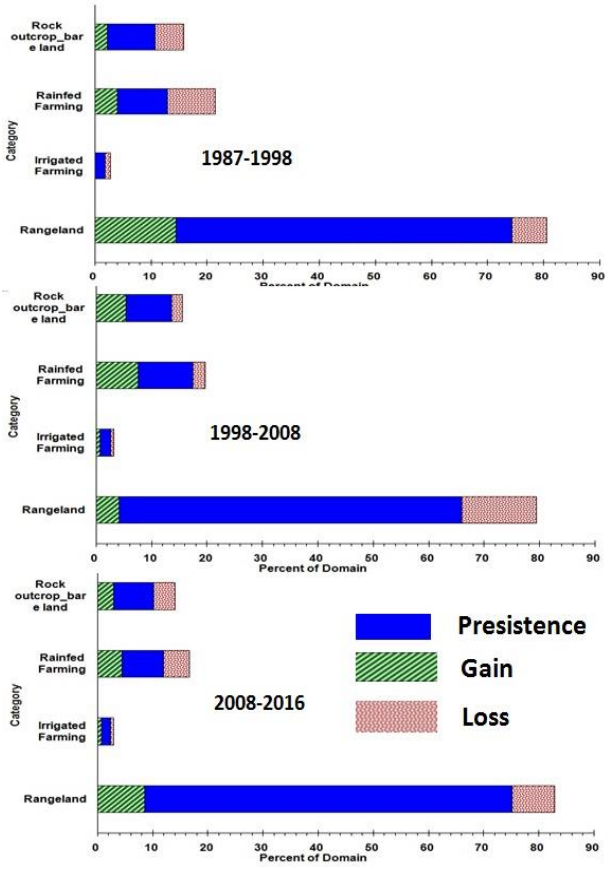

Figure 5. Categorical stationary and Intensity analysis of loss/gain across three time interval

In all time slots, Rangeland accounts for the highest stationary. By comparing different time slots, the middle period 1998-2008 has the highest and the period 1987-1998 has the least stationary. The time interval 1987-1998, the highest gain occurred from the category of Rained Farming to the Rangeland, which could be mainly due to favorable climatic conditions and low population density. During the time interval 1998-2008, the highest loss occurred from the Rangeland category to the rainfed farming category, which can be due to the sudden growth of Mashhad and the increase in the population of this metropolis due to excess migration and consequently increased demand for food from neighboring basins [46, 47].

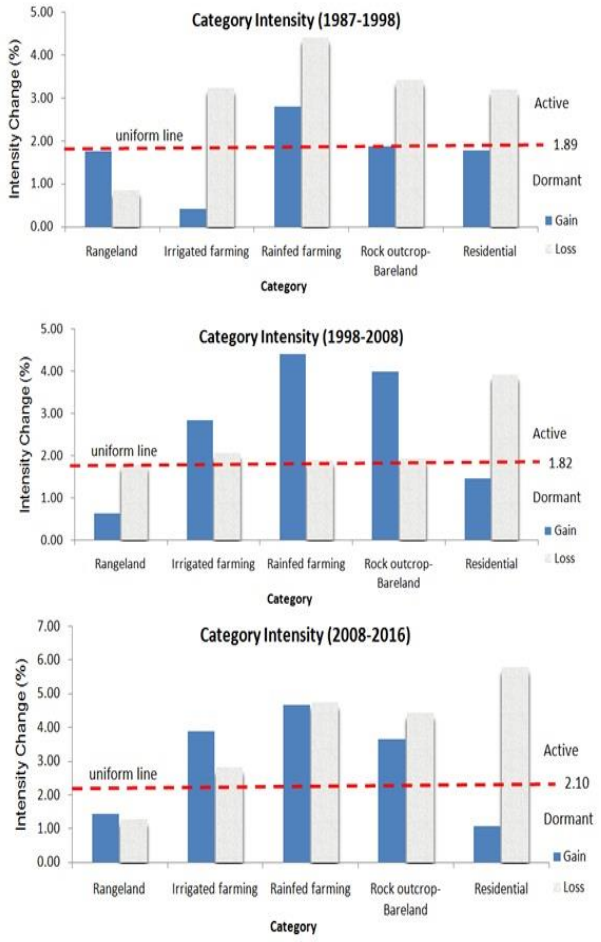

Figure 6. Categorical level intensity analysis during three time intervals

Figure 6 presents the intensity of each category change in each time interval. In each diagram, each category consists of two pairs of bars (Bar), one representing Gain, and another representing Loss. The vertical axis is the intensity of the annual change in percentage. Uniform intensity line indicates the annual changes of the active or inactive variations of each category such that if in the bar diagram, the intensity of the changes in Gain and Loss is less than the uniform line and is positioned at the bottom of that line, then changes in that category would be inactive and dormant, and if it is above the line, the changes would be active.

Rangeland gains and losses and residential gains remained inactive for all the intervals; however, the gains and losses of the irrigated and rainfed farming for 1998-2008 , 2008-2016 and losses of residential area for the three target intervals and only for the losses of irrigated farming in 1987-1998 were active.

The intensity of changes in the Irrigated and Rainfed Farming levels during the period 1998-2008 has the most changes in Gain and Loss. Intense and unprincipled changes of rangelands to Irrigated and Rainfed farmings led to the erosion and increased intensity of Bareland category changes in this period [48-50].

Figures 7 and 8 indicate the intensity of different category changes at any time interval. Each figure has three columns in five lines. The diagrams in the columns indicate the intensity of the category changes in a time interval, while the diagrams of each row represent the changes in the intensity of a category in different time intervals. In Figure 7, if the intensity of the changes in each category is higher than the line of the intensity of the annual changes and is above this line, it means that the changes are significant and are considered as Target. During 1987-1998, the changes in the Rainfed Farming category are significant and changed to the Rangeland category (Target). During the period 1998-2008, changes in the Bareland was significant, and these changes were towards the change into Rangeland. During the time interval 2008 and 2016, the two categories of Rainfed Farming and Bareland, which cut the uniform line of change, have transited to Rangeland. In the time interval 1998-2008 and 2008-2016, the change intensity in the Rainfed Farming category is significant, and the change from this category to the Irrigated Farming category was targeted. Transitions from the rangeland category to Rainfed Farming and Bareland have changed in all time slots.

Figure 8 presents the categories that were targeted in the loss. Categories that are more than the annual uniform intensity line of change and are above this line are significant and considered as the target. During the time period of 1987-1998, the changes in the Rainfed Farming category are significant and are targeted at the Rangeland category, i.e. during this time interval, change was taken place from Rangeland to Rainfed Farming. Changes from the Irrigated Farming category in time interval 1987-1998 to the Rangeland was the target and during 2008-2016 it transited to Rainfed Farming category. During time interval 1987-1998, the change from the Rainfed Farming category was limited to the Rangeland category, however, in the time interval 1998-2008 and 2008-2016, this change was taken place from the Rainfed Farming category to two categories of Irrigated Farming and Rangeland. At all of time intervals, the Bareland category has transited to Rangeland.

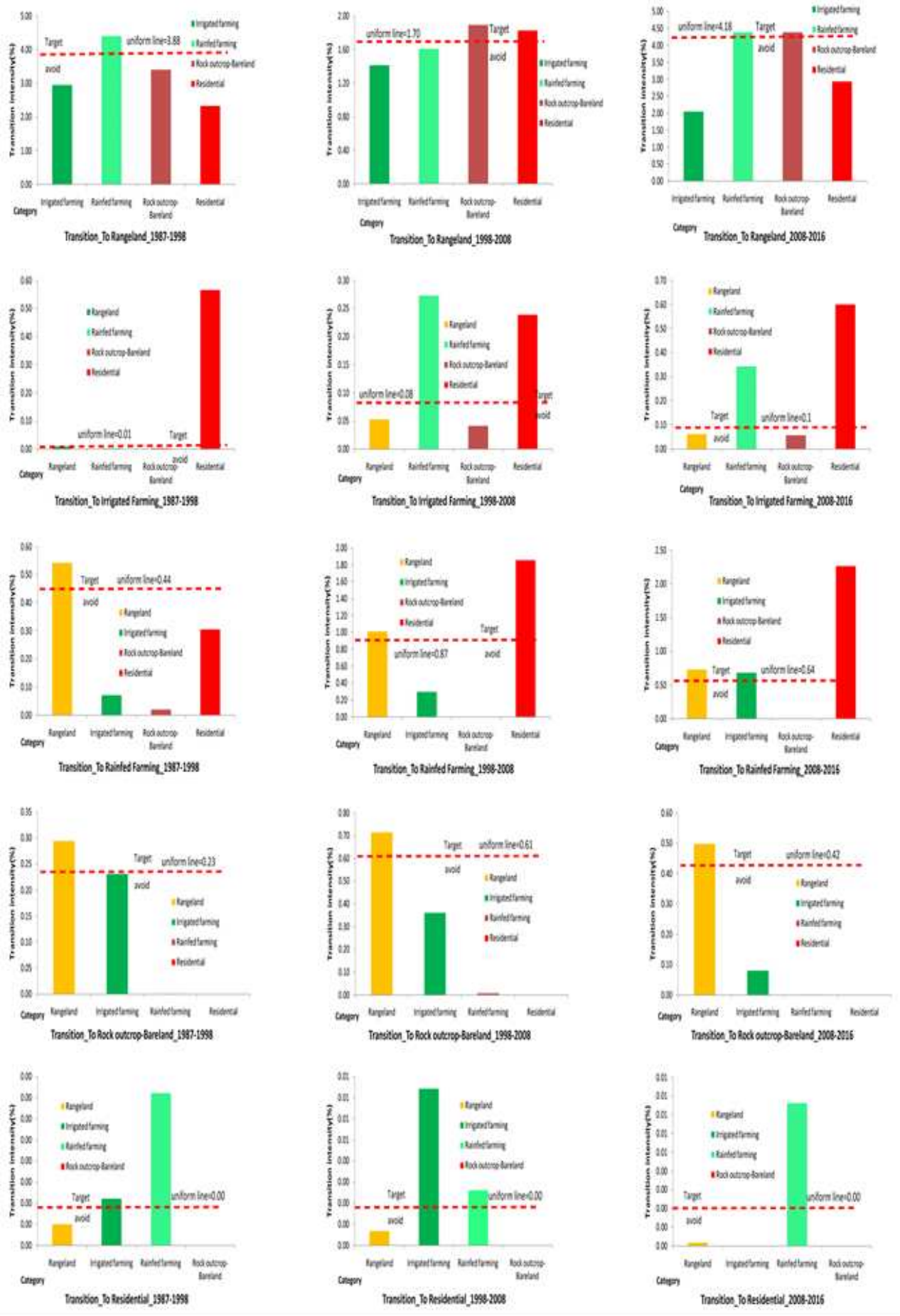

Figure 7 . Transition Intensities represent gaining targets

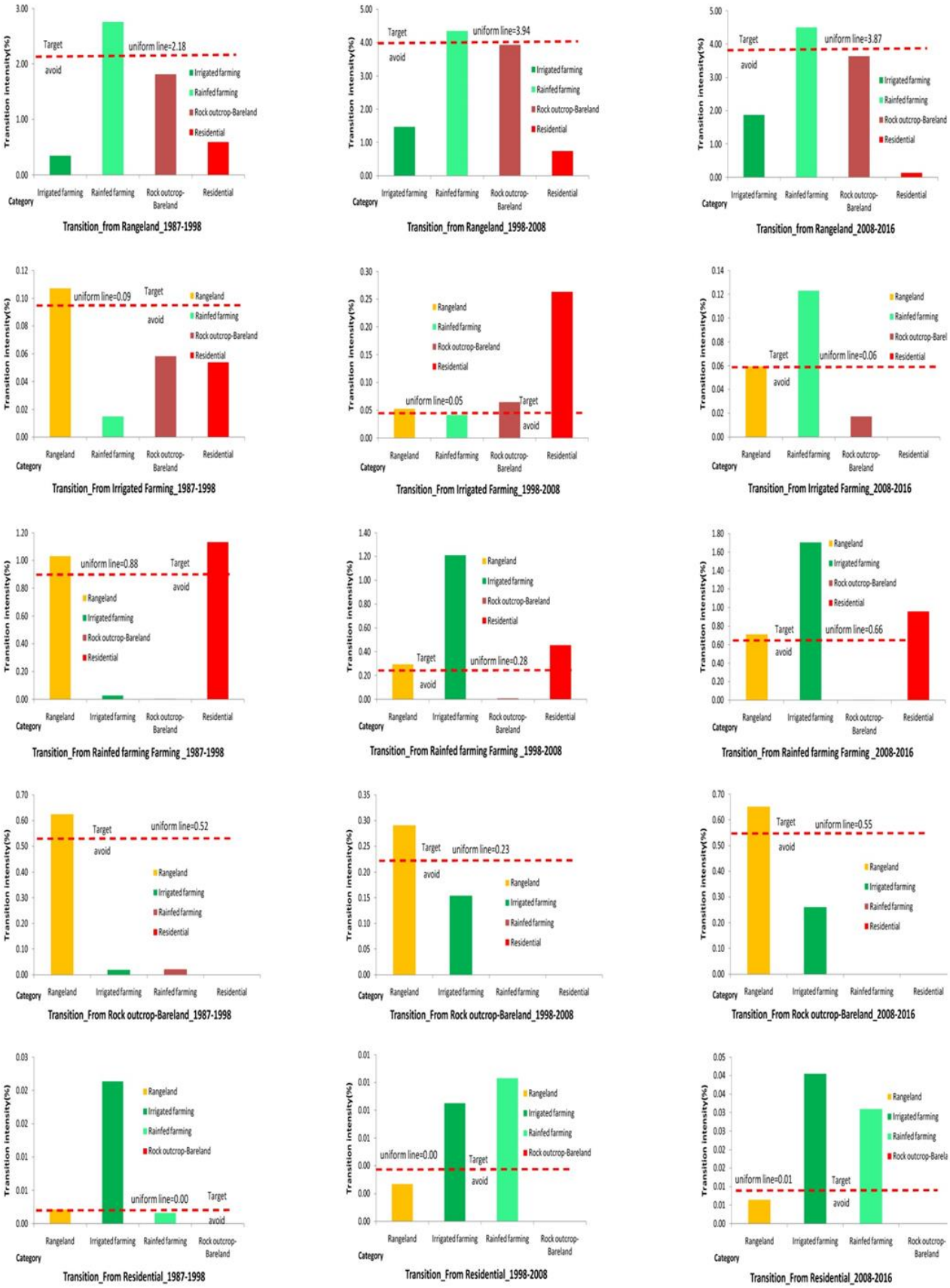

Figure 8. Transition Intensities represent losing targets

Conclusion:

This article analyzes the size and intensity of land use changes and stationary at three levels of time, category and transition intensity. Each level of analysis shows different types of information of changes between categories. In the three studied periods, the results illustrate that the most changes and fluctuations are among the rangeland, irrigated and rainfed farming categories without a regular pattern. Rangeland is the

only dormant category for both gains and losses, in spite of being involved in most of the changes. As the rangeland category has the highest area in this watershed, it plays an important role for being a potential resource for conversion to other uses. The most important reasons are: weaknesses in the enforcement of laws, population growth and the increased demand of food and agricultural activities, development of infrastructure in rural areas such as including electricity which has led to expand pressured irrigation systems for converting rangelands to the rainfed and irrigated farming in high slopes. In the dry years, affected by climate change in Iran, this change would be reversed, and the lands developed to rainfed and irrigated farming, when are not capable in use, have become again to rangeland. These sudden and non-regular changes in the steep slopes have increased the erosion and intensity of the uncovered bare land changes. These types of insights can help other researchers to develop management hypotheses concerning the processes of changes.

References

1. FAO (2008). "A review of drought occurrence and monitoring and planning activities in the Near East region".
2. Whitford, Walter G., Translated by, Azarnivand, Hossein, and Malekian, Arash, 2008, Ecology of desert systems, Tehran: University of Tehran. P. 340.
3. Kirch,B., (2002), "Land Use Impacts on Water Resources," Land and Water Development Division,FAO, Rome Italy,10pp.
4. Sikka A.K., Sarma J.S., Sharda V.N., Samraj P. and Lakshmanam v., (2003). Low flow and high flow responses to converting natural grassland into Bluegum (Eucalyptus globules) in Nilgiris watersheds of south India. Journal of Hydrology, 270: 12-26.
5. Abd El-Kawy,O. R., et al .2011. Land use and land cover change detection in the western Nile delta of Egypt using remote sensing data. Applied Geography, 31(2), 483-494.
6. Bronstert,A., Niehoff,D and Bürger,G. 2002. Effects of climate and land-use change on storm runoff generation: present knowledge and modelling capabilities. Hydrological Processes. 16.2:509-529.
7. Shi, P.J., Yuan, Y., Zheng, J., Wang, J.A., Ge, Y. and Qiu, G.Y., (2007). The effect of land use/cover change on surface runoff in Shenzhen region, China. Catena, 69:31-35.
8. Saghafian, B., Farzjoo, H. Bozorgy, B., and Yazdandoost, F., (2008). Flood intensification due to changes in land use. Water Resource Management. 22, pp. 1051-1067.
9. Brun, S.E., and Band, L. E. (2002). Simulating runoff behaviour in an urbanizing watershed. Computrs Environment and Urban Systems, 24 (1), 5-22.
10. Randhir, T.O.; Hawes, A.G. Watershed land use and aquatic ecosystem response: Ecohydrologic approach to conservation policy. J. Hydrol. 2009, 364, 182–199.
11. Memarian, H., Balasundram, S. K., Talib, J. B., Teh Boon Sung, C., Mohd Sood, A., & Abbaspour, K. C. (2013). KINEROS2 application for land use/cover change impact analysis at the Hulu Langat Basin, Malaysia. Water and Environment Journal, 27(4), 549-560.
12. Turkelboom FT, Poesen J, Trébuil G. The multiple land degradation effects caused by land-use intensification in tropical steeplands: A catchment study from northern Thailand. Elsevier.2008
13. Mawardi I. River Basin Watershed damage and decrease the carrying capacity of water resources in Java as well as efforts to handle (in Indonesian language). Hidrosfir Indonesia Journal; 2010.
14. Schlesinger, W. H., K. H. Reckhow, and E. S. Bernhardt (2006), Global change: The nitrogen cycle and rivers, Water Resour. Res., 42, W03S06.
15. Turner, B. L., II, & Meyer, W. B. (1994). Changes in land use and land cover: A global perspective. In W. B. Meyer, & B. L. Turner (Eds.), Global land-use and land-cover change: An overview (pp. 3–12). Cambridge University Press.
16. Turner, B. L., II. (2002). Toward integrated land-change science: Advances in 1.5 decades of sustained international research on land-use and land-cover change. In W. Steffen, J. Jager, D. J. Carson, & C. Bradshaw (Eds.), Challenges of a changing earth. Proceedings of the Global Change Open Science Conference, Amsterdam, The Netherlands (pp. 21–26). Berlin: Springer.
17. Macleod, R. D., & Congalton, R. G. (1998). A quantitative comparison of changedetection algorithms for monitoring eelgrass from remotely sensed data. Photogrammetric Engineering and Remote Sensing, 64(3), 207–216.
18. McColl,C., Aggett,G. 2007. Land-use forecasting and hydrologic model integration for improved land-use decision support. Journal of environmental management. 84.4: 494-512.
19. Khan, G. A.; Khan, S. A.; Zafar, N. A.; Islam, S.; Ahmad, F.; ur Rehman, M.; Ullah, M., (2012). A review of different approaches of land cover mapping. J. Life Sci. 9(4) (10 pages).
20. Lu, D., Mausel, P., Brondi´zio, E., and Moran, E., (2004). Change detection techniques. INT. J. Remote Sensing, VOL. 25, NO. 12, 2365–2407.
21. Dehvari, A.; Heck, R. J., (2009). Comparison of object-based and pixel based infrared airborne image classification methods using DEM thematic layer. J. Geogr. Region. Plann. 2(4): 86(11 pages).

22. Memarian,H.; Tajbakhsh, M. and S. K. Balasundram, S. K. 2013. "Application of swat for impact assessment of land use/cover change and best management practices: a review," International Journal of Advancement in Earth and Environmental Sciences, vol. 1, no. 1, pp. 36–40.
23. Lillesand, T.M.; Kiefer, R.W.; Chipman, J.W. Remote Sensing and Image Interpretation; John Wiley & Sons Ltd: New York, NY, USA, 2004.
24. Pontius, R.G., Jr.; Malizia, N.R. Effect of category aggregation on map comparison. In Geographic Information Science; Springer: Adelphi, MD, USA, 2004; pp. 251–268.
25. Huang, J.; Pontius, R.G., Jr.; Li, Q.; Zhang, Y. Use of intensity analysis to link patterns with processes of land change from 1986 to 2007 in a coastal watershed of southeast China. Appl. Geogr. 2012, 34, 371–384
26. Aldwaik, S.Z.; Pontius, R.G., Jr. Intensity analysis to unify measurements of size and stationarity of land changes by interval, category, and transition. Landsc. Urban Plan. 2012, 106, 103–114
27. Pontius, R.G., Jr.; Shusas, E.; McEachern, M. Detecting important categorical land changes while accounting for persistence. Agric. Ecosyst. Environ. 2004, 100, 251–268.
28. Azami Rad, M.; Saeedian, F. 2010. Investigate the flood probability in terms of infiltration and runoff in geology formations in the Kardeh Catchment Basin.
29. Osgouei, P. E., & Kaya, S. (2017). Analysis of land cover/use changes using Landsat 5 TM data and indices. Environmental monitoring and assessment, 189(4), 136.
30. Duong, N. D. (2016). Automated Classification of Land Cover Using Landsat 8 Oli Surface Reflectance Product and Spectral Pattern Analysis Concept-Case Study in Hanoi, Vietnam. International Archives of the Photogrammetry, Remote Sensing & Spatial Information Sciences, 41.
31. Emre Tekel A. , 2005: Operational hydrological forecasting of snowmelt runoff by remote sensing and geographic information systems integration.
32. Wang, Z. et al., "Object-oriented classification and application in land use classification using SPOT-5 PAN imagery," in Geosci. Rem. Sens. Symp., Vol. 5, pp. 3158–3160 (2004).
33. Dean, A. M.; Smith, G. M., (2003). An evaluation of per-parcel land cover mapping using maximum likelihood class probabilities. Int. J. Rem. Sens. 24(14): 2905-2920 (16 pages).
34. Richards, J. A.; Jia, X., (2006). Remote Sensing Digital Image Analysis, 4th ed., Springer-Verlag, Berlin, Heidelberg.
35. Rees, G., (1999). The remote sensing data book. Cambridge University press (271 pages).
36. Brandt, T. and Mather P.M. 2001: Classification methods for remotely sensed data. Taylor & Francis, Londen and newyork, 210 p.
37. Akbarpour, A.; Sharifi, M. B.; Memarian, H., (2006). The comparison of fuzzy and maximum likelihood methods in preparing land use layer using ETM+ data (Case study: Kameh watershed), Iran. J. Range Desert Res. 13(1): 27–38 (12 pages) (In Persian).
38. Richards, J. A., & Richards, J. A. (1999). Remote sensing digital image analysis (Vol. 3). Berlin et al.: Springer.
39. Mather, P.M. 1999: Computer Processing of Remotely-sensed Images, John Wiley & Sons.New York, 332 p.
40. Zhou, P., Huang, J., Pontius R. G., and Hong, H. 2014. "Land Classification and Change Intensity Analysis in a Coastal Watershed of Southeast China". International Journal of Sensors 14(7): 11640-11658 .
41. Pontius, R. G., Gao, Y., Giner , N., Kohyama, T., Osaki, M. , and Hirose, K. 2013. "Design and Interpretation of Intensity Analysis Illustrated by Land Change in Central Kalimantan, Indonesia". International Journal of Lands 2, 351-369.
42. Viera, A. J., & Garrett, J. M. (2005). Understanding interobserver agreement: the kappa statistic. Fam med, 37(5), 360-363.
43. Tajbakhsh, M., Memarian, H., & Shahrokhi, Y. (2016). Analyzing and modeling urban sprawl and land use changes in a developing city using a CA-Markovian approach. Global Journal of Environmental Science and Management, 2(4), 397-410.
44. Sayari, N., Bannayan, M., Alizadeh, A., & Farid, A. (2013). Using drought indices to assess climate change impacts on drought conditions in the northeast of Iran (case study: Kashafrood basin). Meteorological Applications, 20(1), 115-127.
45. Rahim Rahnama, M., Homaeefar, A., & Piruz, T. (2013) Evaluating of Mashhad urban development plans from compact city viewpoint. American Journal of Engineering Research (AJER), 2(9), 208-213.
46. Motlaq, M. A., & Abbaszadeh, G. (2012). The physical development of Mashhad city and its environmental impacts. Environment and Urbanization ASIA, 3(1), 79-91.
47. Saeidian, F., Sulaiman, W. N. A. B., & Rad, M. A. (2009). The Investigation of the Sediment Yield Potential Using Hydro-Physical Method in the Drainage Basins (Case Study in Kardeh Drainage Basin-Iran). Global Journal of Environmental Research, 3(3), 178-186.
48. Naseri, S., Jafari, M., Tavakoli, H., & Arzani, H. (2014). Effects of mechanical erosion control practices on soil and vegetation carbon sequestration (case study: Catchment Basin of Kardeh-Iran).

49. Golrang, B. M. (2017). Mixed-Method Evaluation of Watershed Management: Practices from Kushk-Abad Basin, Iran. Springer.
50. Memarian, H., Balasundram, S. K., & Khosla, R. (2013). Comparison between pixel-and object-based image classification of a tropical landscape using Système Pour l'Observation de la Terre-5 imagery. Journal of Applied Remote Sensing, 7(1), 073512.